applied optics

Influence of substrate temperatures on the properties of GdF_3 thin films with quarter-wave thickness in the ultraviolet region

Jingcheng Jin, Chunshui Jin,* Chun Li, Wenyuan Deng, and Shun Yao

State Key Laboratory of Applied Optics, Changchun Institute of Optics, Fine Mechanics and Physics, Chinese Academy of Sciences, Changchun, Jilin 130033, China
**Corresponding author: jin_chunshui@aliyun.com*

Received 21 January 2015; revised 16 April 2015; accepted 20 April 2015; posted 20 April 2015 (Doc. ID 232725); published 28 May 2015

High-quality coatings of fluoride materials are in extraordinary demand for use in deep ultraviolet (DUV) lithography. Gadolinium fluoride (GdF_3) thin films were prepared by a thermal boat evaporation process at different substrate temperatures. GdF_3 thin film was set at quarter-wave thickness (~27 nm) with regard to their common use in DUV/vacuum ultraviolet optical stacks; these thin films may significantly differ in nanostructural properties at corresponding depositing temperatures, which would crucially influence the performance of the multilayers. The measurement and analysis of optical, structural, and mechanical properties of GdF_3 thin films have been performed in a comprehensive characterization cycle. It was found that depositing GdF_3 thin films at relative higher temperature would form a rather dense, smooth, homogeneous structure within this film thickness scale.

OCIS codes: (260.7210) Ultraviolet, vacuum; (310.6628) Subwavelength structures, nanostructures; (160.4670) Optical materials; (310.6860) Thin films, optical properties.

http://dx.doi.org/10.1364/AO.54.005117

1. INTRODUCTION

The use of excimer lasers extending to deep/vacuum ultraviolet (DUV/VUV) wavelengths is increasing in semiconductor applications, material microstructuring, and medical surgeries because of their high power, high homogeneity, and high stability [1]. Such excimer lasers are being developed for higher output power, repetition rates, enhancements on beam homogeneity, and pulse stability, feeding an ever-growing demand for the coating components working at this wavelength range [2–5]. Manufacturing high-quality optical coatings for applications in the UV region requires reliable property characterization of the thin films.

However, only a few fluoride materials can be employed in the DUV/VUV region due to their unrivaled position as a large-bandgap material. Among the very limited number of materials, besides LaF_3, GdF_3 is a potential high refractive index candidate for further development in the excimer laser application area. Furthermore, these fluoride materials have the potential for application in the UV region down to 130 nm [3,6]. It was shown that the least amount of optical loss of the fluoride can be obtained by resistive heating evaporation. Different substrates such as fused silica or CaF_2 would be chosen due to various application conditions; GdF_3 thin films grown on different substrates may exhibit different properties. However, the influence of substrate type is not in the scope of this paper. The substrate temperature is regarded as the most relevant depositing parameter ruling the microstructure of the deposited films. As a high refractive index material, GdF_3 was believed to be responsible for the main cause for scattering and absorption loss in the multilayer stacks.

Pioneering work has been done to evaluate the optical and structural properties of the evaporated GdF_3; however, the physical property results of GdF_3 thin films in the UV spectral range are dissimilar [7–10]. The value of the refractive index of GdF_3 film is usually thickness dependent because of its inhomogeneous structure. Due to the fact that the thickness used for analysis is usually hundreds of nanometers does not correspond to the common geometrical thickness of the films in DUV/VUV optical multilayer stacks. Thus, GdF_3 films with thickness around 27 nm was deposited on fused silica under different substrate temperatures by thermal evaporation in our research, which is much closer to the expected real geometrical cases. The case of wavelength equal to 193 nm is used as an example in the following illustration and analysis.

The optical properties, crystalline structure, microstructure, and mechanical characteristics of the deposited GdF_3 thin films

were analyzed and compared. The variation trends in microstructures of GdF_3 thin films versus substrate temperatures is an eye guide for the extrapolation of the usability in the DUV/VUV multilayer stacks, which is helpful to verify functionalities and to understand possible performance changes during the multilayer stack deposition.

2. EXPERIMENTS

GdF_3 thin films were deposited using the Ta boat evaporation method in a Leybold SYRUSpro 1110 DUV batch coater. The chamber was pumped out to a base pressure less than 2×10^{-6} Pa before the evaporation process. Superpolished fused silica (RMS < 0.5 nm) was used as a substrate. The substrates and the chamber were conditioned with a reactive plasma pretreatment. This pretreatment was applied to remove residual water vapor and hydrocarbons. The deposition temperatures were 150°C, 250°C, 300°C, 350°C, and 380°C. Deposition rate, controlled by a quartz crystal sensor, was set to 0.2 nm/s.

The films were evaluated by variable angle spectroscopic ellipsometry (SE5-PUV, Sopra). The ellipsometric parameters psi (ψ) and delta (Δ) were obtained by the ellipsometer with a rotating analyzer. The sample holder and the detectors were mounted on precision goniometers, which gave an angular resolution of 0.01°. Purged with high-purity nitrogen, the measurement was performed in the spectral range from 160 to 230 nm at an incidence angle of 62° for sensitive consideration at the given thickness.

The laser calorimeter (Laser Zentrum Hannover) was used to determine the extinction coefficients of the thin films. The absorption test of GdF_3 thin films was carried out in the laser calorimeter system by using normal incidence of the ArF laser beam. The irradiation was carried out at the wavelength of 193 nm with a fluence of 1.58 mJ/cm^2 and a repetition rate of 1 kHz. The heating and cooling times were set to 120 and 560 s, respectively. The extinction coefficients were calculated from the heating and cooling temperature curves [11].

The microstructure of GdF_3 films were assessed by x-ray diffraction (XRD) (PANalytical X'pert), equipped with a Cu-Ka radiation source ($\lambda = 0.15418$ nm). Diffraction angle 2θ varied from 20° to 60°, stepped by 0.05°. Direct comparisons of diffraction intensity were made in order to evaluate differences in the degree of crystallization between samples deposited at different temperatures. The average crystal diameters of GdF_3 films were estimated from the Scherrer's equation for the microstructure analysis.

The surface roughness RMS of GdF_3 was evaluated by atomic force microscopy (AFM) (Nanosurf Easyscan 2) with sampling range 1 μm × 1 μm, 10 μm × 10 μm, and sampling points 256 × 256. The spatial-frequency range of the power spectrum density (PSD) function, which is related to the total scattering (TS) for the UV range, was applied for the roughness analysis.

The mechanical stress of the films was derived from the deformation of a silicon wafer due to the deposited films before and after the coating in a mechanical stress measurement device (FSM 500TC). Details of the procedure to evaluate the stress of the films are given in [12].

3. RESULTS AND DISCUSSION

A. Optical Analysis

Spectroscopic ellipsometry is a sensitive and nondestructive measurement technique in the UV spectral region for determination of the physical thickness and optical constants [10,13]. The combination of variable angle of incidence and spectroscopic measurements allows one to select the most sensitive spectral acquisition range and angles of incidence. A proper structural model enables one to fit spectroscopic ellipsometer data with a small deviation. A modified Cauchy formula is used to represent the GdF_3 dispersion model.

The experimental data and fitted results at an angle of incidence of 62° by assuming a homogeneous GdF_3 layer on the fused silica surface is shown in Fig. 1; the measured data are labeled *M*, whereas the fitted data are labeled *F*. The layer thickness obtained from regression results is 26.8 nm with a mean squared error (MSE) of $\sim 2.4 \times 10^{-4}$. The error budgets of refractive index and thickness were believed to be lower than 0.005 and 1 nm, respectively.

The MSE indicates the extent of consistency between the constructed model and the actual GdF_3 film. Additional attempts were accomplished by applying an inhomogeneous model and showed no further improvement on MSE, which suggests that the refractive index of the GdF_3 film is independent of the layer thickness because of its homogeneous structure.

The extensive reported inhomogeneity of GdF_3 was undetectable during this first 27 nm growth [7–10]. The inhomogeneity of GdF_3 film is a result of the film porosity change as film thickness accumulatively increases; the growth mechanisms of cone-shaped columnar and polycrystalline microstructures may introduce gaps between the grains, leaving a discontinuous columnar structure with more voids between the microstructures. As a consequence, the film packing density decreases as the layer thickness accumulates; this phenomenon explains why different refractive indices of GdF_3 films are reported in the literatures, depending not only on deposition conditions but also on the film thickness used for optical index extraction.

The refractive index of GdF_3 films deposited at specific depositing temperatures are shown in Table 1. As is shown in

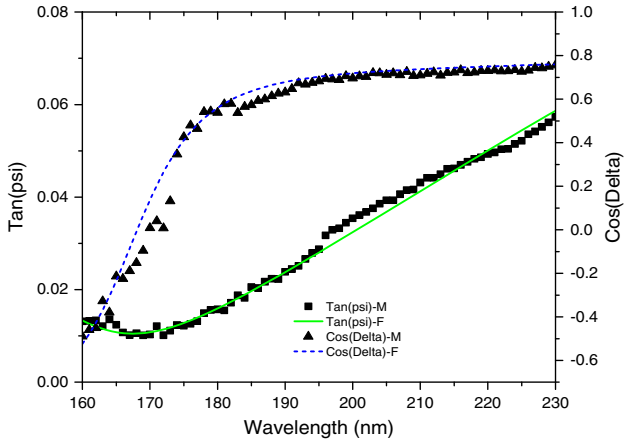

Fig. 1. Fitting spectral data of ellipsometry of GdF_3 layer.

Table 1. Refractive Index of GdF_3 Films at Specific Depositing Temperatures

Temperature (°C)	n@193 nm	D (nm)	MSE (10-4)
150	1.681	27.2	2.66
250	1.709	27.1	2.64
300	1.718	26.8	2.37
350	1.725	27.4	2.16
380	1.726	27.1	2.25

Table 1, higher depositing temperatures lead to a higher refractive index from 150°C to 380°C. Due to the lower packing density of GdF_3 films grown at 150°C, the refractive index of such films is much lower than the refractive index of a film grown at 350°C or above. The highest refractive index reached 1.726 ($\lambda = 193$ nm) at the temperature of 380°C.

The extinction coefficients calculated from laser calorimetry measurements revealed the influence direction of optical absorption loss versus depositing temperature. As demonstrated in Fig. 2, higher depositing temperature lead to a lower extent of absorption loss (dashed line). The minimal absorption loss of GdF_3 films happened at the substrate temperature around 350°C–380°C, with an extinction coefficient of approximately 0.003 ($\lambda = 193$ nm).

The influence of depositing temperature on the optical constant is obvious. The result suggests that depositing temperature plays a critical role in the GdF_3 film growth mechanisms. This phenomenon arises because the mobility of GdF_3 molecules is particularly sensitive to the temperature of substrates. The effect of increasing kinetic energy of the depositing molecules influences the film microstructures and packing density and thus the refractive index and extinction coefficient values. Thus, the detailed study of the grown states and microstructural properties of GdF_3 films was carried out as discussed in the following sections.

B. Microstructures

The growth structure zone model of films as a function of T_s/T_m (where T_s is the substrate temperature and T_m is the melting temperature of the material; T_m of GdF_3 is 1231°C) was applied to interpret the microstructures of GdF_3 thin films [14]. The mobility of GdF_3 molecules is particularly sensitive to the temperature of substrates. According to this zone model, there are four kinds of microstructures associated with four different temperature zones:

Zone I: $T_s/T_m \le 0.15$
Zone T: $0.15 < T_s/T_m \le 0.3$
Zone II: $0.3 < T_s/T_m \le 0.5$
Zone III: $T_s/T_m > 0.5$

Depositing temperature from 150°C to 380°C covers three structure growth zones from Zone I to Zone II. The XRD patterns of the samples deposited at various substrate temperatures are shown in Fig. 3. These patterns suggest that the GdF_3 film has a polycrystalline structure. The diffraction peaks of the coatings match well with the GdF_3 orthorhombic structure.

When the substrate temperature was 150°C, the T_s/T_m ratio of the GdF_3 films is 0.123, which belongs to Zone I. In Zone I, because of limited surface diffusion and atomic shadowing effects, the film was extensively porous, and the packing density was low. As illustrated in Fig. 3, when the substrate temperatures was 150°C, only the (101) and (020) diffraction peaks were detected, which might be due to the low mobility of evaporated GdF_3.

When the substrate temperature increased to 250°C and 300°C, the T_s/T_m ratios are 0.203 and 0.243, respectively, which places them in Zone T. In Zone T, the microstructures of the films are cone-shaped columnar structures due to the effect of molecular migration and surface diffusion as the films grow. The (101), (020), (111), (112), and (301) crystalline structures had been detected at substrate temperatures of 250°C and 300°C. The intensity ratio of $I(101)/(020)$ at the substrate temperature of 300°C was larger than that at 250°C because higher heat energy leads to a more oriented crystalline structure. This indicates that the crystallization status of orthorhombic GdF_3 becomes better as the substrate temperature increases.

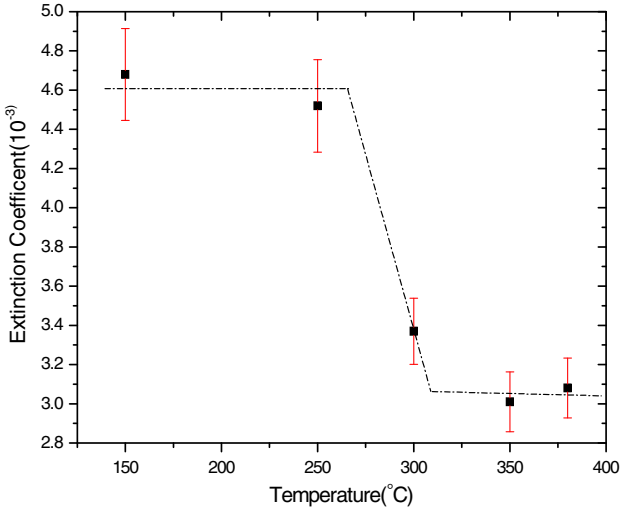

Fig. 2. Extinction coefficient of GdF_3 films at different depositing temperatures.

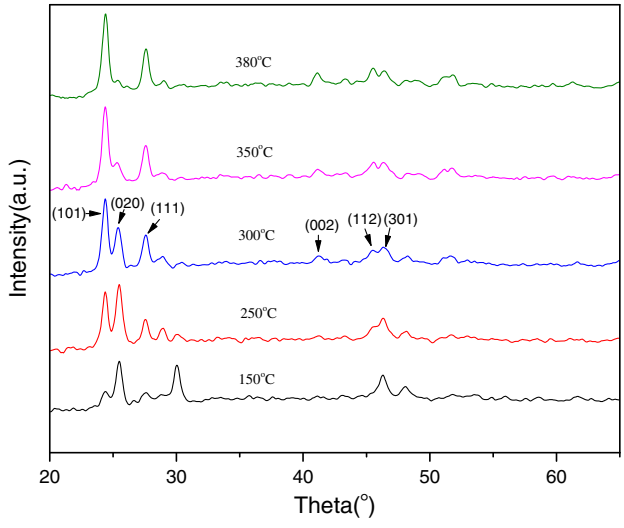

Fig. 3. XRD patterns from GdF_3 films at different depositing temperatures.

Table 2. Average Crystal Diameters of GdF_3 Films at Different Deposition Temperatures

Temperature (°C)	2θ (°)	β (°)	D (nm)
150	25.50	0.48	16.99
250	25.44	0.41	19.88
300	25.50	0.38	21.49
350	24.40	0.44	18.51
380	24.36	0.48	16.96

At 350°C the ratio reaches 0.284, which was very close to the initial temperature region of Zone II, exhibiting similar characteristic as at 380°C and possessing obvious microstructures of Zone II. In Zone II, volume diffusion and grain boundary migration start to operate in addition to surface diffusion; the column microstructures of GdF_3 films in Zone II have fewer voids than those in Zone T. The effect of increasing heat supplies thermal energy of molecules and enhances the microstructures and packing density. The strongest intensities of I (101) was detected at the temperature of 380°C; this is because high heat energy will lead to a more oriented crystalline structure. The (101) fiber texture is already well existent in very thin films of only about 27 nm.

Table 2 shows the average crystal diameters of evaluated GdF_3 films at specific deposition temperatures, where β is the full width of peaks at half maximum intensity. These numbers give the average dimension of the grains in the film in the growth direction. Obviously, the average crystal diameters increased with the temperature elevating from 150°C to 300°C, then decreased when the substrate temperature reached 350°C–380°C. It is clear that the size of GdF_3 deposition molecule groups at the substrate temperature of 250°C–300°C is larger than that at 150°C.

The film was composed of fibers of small diameter that increased with substrate temperature from Zone I to Zone T. The size of the cone-shaped columnar structure was increased when the substrate temperature was elevated in Zone T; the phenomenon gradually faded in Zone II, perhaps owing to the exchange of the cone-shaped columnar structure for the column microstructure. The elevation of substrate temperature to 350°C and above led to a pronounced development of a fiber texture of the (101) crystallites planes parallel to the substrate surface as confirmed by XRD patterns.

C. Roughness Characterization

The AFM was employed to analyze the surface microstructure with a scanning area of 10 μm × 10 μm, 1 μm × 1 μm with 256 × 256 data points, respectively. The AFM images clearly reveal the nanoporous morphology of GdF_3 film growth on a fused silica surface.

Even though direct scatter measurements were not performed, the different roughness levels suggest different scatter losses depending on the deposition temperature. The RMS roughness results of GdF_3 films given in Fig. 4 increased as substrate temperatures elevated from 150°C to 250°C, then decreased from 300°C to 380°C. The minimum value of RMS roughness happened at a substrate temperature of 380°C. The RMS roughness of the GdF_3 films grown at the temperature of 350°C and 380°C was found to be about 0.7 nm,

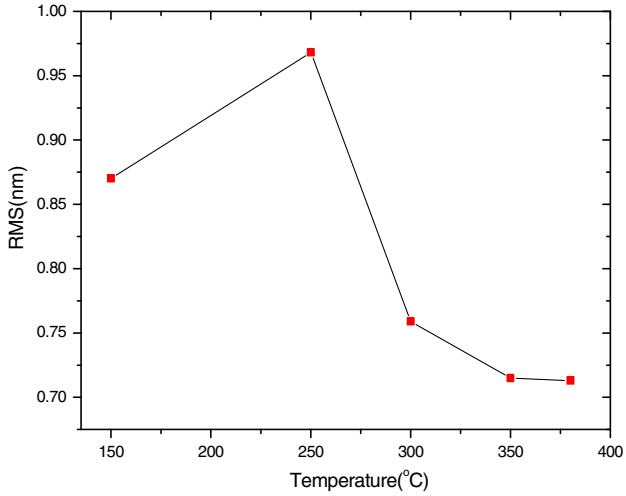

Fig. 4. RMS-roughness of GdF_3 films deposited at different temperatures.

which is slightly higher than the substrate roughness, while a value of about 0.76 nm was determined for the 300°C sample, which is lower than the value for 250°C and 150°C.

As can be seen in the 1 μm × 1 μm image in Fig. 5, there are some gaps between the accumulated dense grains, leading to the formation of a porous structure. The morphology of thin films critically affects the performance of the optical components, so the spatial-frequency range of the PSD function, which is related to the TS for the UV range, was applied to characterize surface roughness. The corresponding spatial-frequency range for 193 nm is 0.181–5.162 μm^{-1}, and the average PSDs calculated from several single measurements for each film is used to reduce the impact of statistical noise [15–17]. Depositing temperatures from 150°C to 380°C cover three structure growth zones, so three representational examples (150°C, 300°C, and 380°C) are given for morphology analysis.

The PSD results as shown in Fig. 6 indicate a superposition of different growth morphologies affecting different spatial frequency ranges. GdF_3 films fabricated in separate structure zones have different spatial frequency features. GdF_3 film deposited at 300°C exhibits the highest PSDs in the low-spatial-frequency region below 0.4 μm^{-1}. This reveals the fact that more cusplike features with bigger diameter were formed at 300°C than at 150°C and 380°C, which is also observable in the AFM image. The PSD behaviors were similar in the mid-spatial-frequency regions (0.4–2 μm^{-1}), which indicates the grain coverage of the corresponding sizes were quite alike. In the high-spatial-frequency range (2–6 μm^{-1}), GdF_3 films are smoother when deposited at 300°C and 380°C than at 150°C; this is presumably the result of a denser columnar growth with fewer tiny peaks. Therefore, the development of surface roughness of GdF_3 grown at high temperatures is expected for smoother components in multilayer stack manufacturing.

D. Mechanical Stress

The stress of a thin film is basically related to the chemical composition of the film and to the morphological and crystalline structures developed during the growth. The mechanical stress

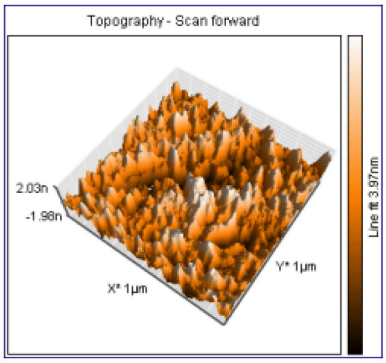

(a) 150°C

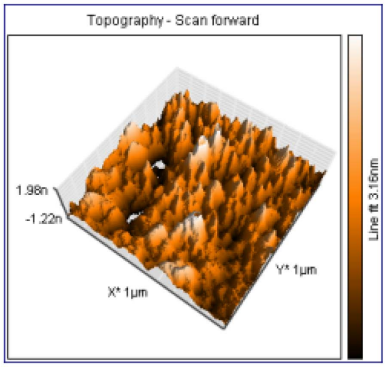

(b) 300°C

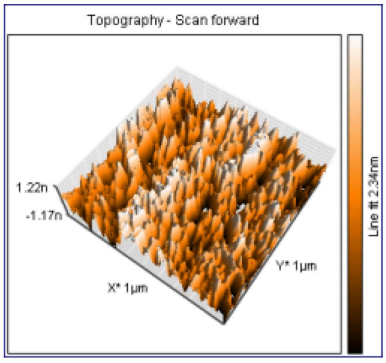

(c) 380°C

Fig. 5. Surface morphology of GdF_3 thin films of different depositing temperatures measured by AFM (1 μm × 1 μm).

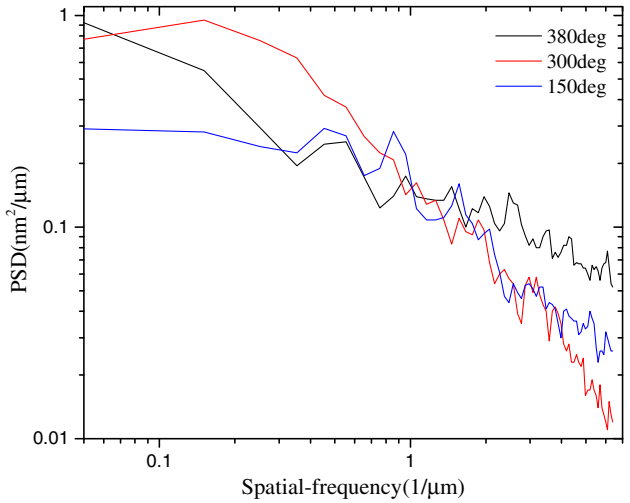

Fig. 6. PSDs of GdF_3 films deposited at different temperatures.

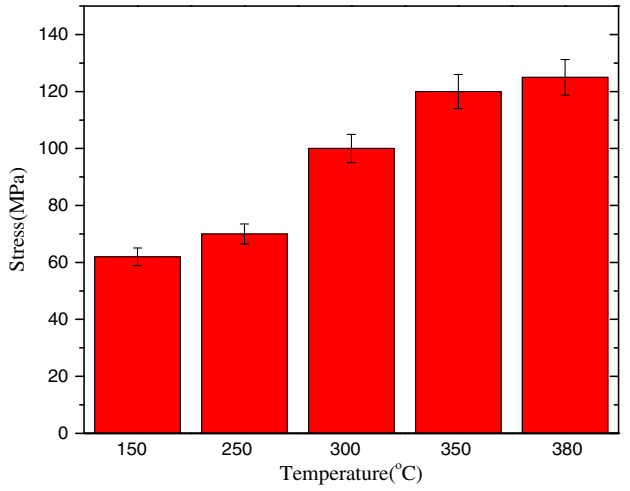

Fig. 7. Stress of GdF_3 films deposited at different temperatures.

is strongly influenced by the deposition conditions and is especially sensitive to depositing temperatures.

In the mechanical stress evaluations, a laser deflection method for the detection of stress-induced sample bending is used. The absolute stress measurements were carried out immediately after the deposition was finished, and the mechanical stress of the GdF_3 thin films was derived from the deformation of substrates due to the deposited films before and after the coating. Figure 7 shows the stress of GdF_3 films deposited at different temperatures by using Stoney's equation [12]; independent of the substrate temperature all the GdF_3 films exhibited tensile stress values between 62 and 125 MPa. The GdF_3 thin films deposited at a higher substrate temperature show slightly higher tensile stress due to the larger thermal expansion coefficient difference between the GdF_3 thin films and the substrates. The mechanical properties of the thin films are mainly determined by the growth-zone characteristics. However, the stress-induced damage often results in the destruction of optical components due to crack formation of the coatings; thus the noticeably large stress of GdF_3 thin films at higher temperature has to be considered for mechanical stability limitation in the multilayer stack fabrication.

4. CONCLUSIONS

Various microstructures of GdF_3 thin films with typical thickness for the DUV/VUV range that were formed under different substrate temperatures were investigated. The results showed that depositing GdF_3 thin films at a relative high substrate temperature (350°C–380°C) will form a rather homogeneous and smoother structure along the film thickness. The effect of increasing heat supplies will improve crystallization status and increase the packing density and tensile stress inside the film,

causing a low optical absorption loss and a high refractive index. The key to high-quality UV coatings is the detailed understanding of the intrinsic properties of the candidate materials and the interrelationship of the physical properties with deposition conditions. The influence of depositing temperature on the structural properties of GdF_3 is the extrapolation of practical application in multilayer stacks at the UV region, which is helpful to understand possible performance fluctuations during the multilayer stack deposition. Similar research on other substrates, such as CaF_2, is also significant and essential for future work.

REFERENCES

1. D. Basting, G. Marowsky, and U. Brinkmann, *Excimer Laser Technology* (Springer Berlin Heidelberg, 2005).
2. R. Biro, K. Sone, S. Niisaka, M. Otania, Y. Suzuki, C. Ouchi, T. Saito, M. Hasegawa, J. Saito, A. Tanaka, and A. Matsumoto, "Development of low-loss optical coatings for 157 nm lithography," Proc. SPIE **4691**, 1625–1634 (2002).
3. C. Zaczek, S. Mullender, H. Enkisch, and F. Bijkerk, "Coatings for next generation lithography," Proc. SPIE **7101**, 71010X (2008).
4. J. Jin, C. Jin, C. Li, and Y. Chang, "Fabrication anti-reflection (AR) coatings for polarized 193 nm laser light at an incidence angle of 74°," Opt. Commun. **298**, 171–175 (2013).
5. J. Jin, C. Jin, C. Li, W. Deng, and Y. Chang, "Optimal design and fabrication method for antireflection coatings for P-polarized 193 nm laser beam at large angles of incidence (68°–74°)," J. Opt. Soc. Am. A **30**, 1768–1771 (2013).
6. T. Yoshida, K. Nishimoto, K. Sekine, and K. K. Etoh, "Fluoride antireflection coatings for deep ultraviolet optics deposited by ion-beam sputtering," Appl. Opt. **45**, 1375–1379 (2006).
7. M. C. Liu, C. C. Lee, M. Kasaaki, K. Nakahira, and Y. Takano, "Microstructure-related properties at 193 nm of MgF_2 and GdF_3 films deposited by a resistive-heating boat," Appl. Opt. **45**, 1368–1374 (2006).
8. S. Schröder, H. Uhlig, A. Duparré, and N. Kaiser, "Nanostructure and optical properties of fluoride films for high-quality DUV/VUV optical components," Proc. SPIE **5963**, 59630R (2005).
9. R. Thielsch, J. Heber, H. Uhlig, and N. Kaiser, "Optical, structural and mechanical properties of gadolinium tri-fluoride thin films grown on amorphous substrates," Proc. SPIE **5963**, 59630O (2005).
10. J. Wang, R. Maier, P. G. Dewa, H. Schreiber, R. A. Bellman, and D. D. Elli, "Nanoporous structure of a GdF_3 thin film evaluated by variable angle spectroscopic ellipsometry," Appl. Opt. **46**, 3221–3226 (2007).
11. "Test method for absorptance of optical laser components," ISO/FDIS 11551, 1995.
12. R. Thielsch, J. Heber, H. Uhlig, and N. Kaiser, "Development of mechanical stress in fluoride multi-layers for UV-applications," Proc. SPIE **5250**, 127–136 (2005).
13. J. N. Hilfiker, C. L. Bungay, R. A. Synowicki, T. E. Tiwald, C. M. Herzinger, B. John, G. K. Pribil, and J. A. Woollam, "Progress in spectroscopic ellipsometry: applications from vacuum ultraviolet to infrared," J. Vac. Sci. Technol. A **21**, 1103–1108 (2003).
14. A. Movchan and A. V. Demchishin, "Study of the structure and properties of the vacuum condensation of nickel, titanium, tungsten, aluminum oxide, and zirconium dioxide," Fiz. Met. Metalloved. **28**, 653–660 (1969).
15. J. Ferré-Borrull, A. Duparré, and E. Quesnel, "Roughness and light scattering of ion-beam-sputtered fluoride coatings for 193 nm," Appl. Opt. **39**, 5854–5864 (2000).
16. S. Schröder, M. Kamprath, and A. Duparré, "Scatter analysis of optical components from 193 nm to 13.5 nm," Proc. SPIE **5878**, 58780T (2005).
17. S. Schröder, A. Duparré, and A. Tünnermann, "Roughness evolution and scatter losses of multilayers for 193 nm optics," Appl. Opt. **47**, C88–C97 (2008).